

Flexible Packaging Division Newsletter Summer 2016 edition

July 31, 2016

FLEXIBLE PACKAGING: FlexPackCon 2016

With AIMCAL Conference

October 9-12, 2016
Peabody Hotel
Memphis, TN



Information &
Registration:
4spe.org/flexpackcon2016



FLEXIBLE
PACKAGING

Flex Pack at ANTEC, May 2016

All-star Line Up

1. *Tutorial: Long Chain Branched / High Melt Strength Linear Low Density Polyethylene for Blown and Cast Film Applications*
Edward Phillips, Polyolefins Specialist
2. *Coating Trials for an Antimicrobial Coating Containing Nisin 2.5% Using Gravure and Flexographic Converting Processes*
Michele Perna, Ph.D. Student, Clemson U. [Bemis]
3. *Predicting the Impact Structure Response of Multilayer Flexible Food Packages Using Explicit Finite Element Models*
Barry Morris, Technical Fellow, DuPont
4. *Capillary Coextrusion: A New Process for Creating Small-scale Coextruded Films*
Patrick Lee, Assistant Professor, U. of Vermont
5. *Case Studies of PP Based olefin block copolymers (OBC) for Multilayer Packaging*
Yushan Hu, The Dow Chemical Company
6. *Agility Performance LDPE as a Blend Component in High Throughput and High Bubble Stability Blown Film Applications*
Teresa Karjala, The Dow Chemical Company

And the “Division best paper” winner is:

Barry Morris of DuPont. His paper is included in the following pages.

SPE Fellows

Two Division Nominees Named SPE Fellows in Recognition of their Plastic Engineering and Applications Achievements

The division nominated Tom Dunn from the Flexible Packaging Division and Dr. Luyi Sun from the Engineering Properties and Structure Division. Both nominees received the recognition at the 2016 ANTEC SPE Awards Gala held Sunday, May 22nd in Indianapolis.

Tom Dunn: Managing Director, Flexpacknology, LLC.

Tom Dunn is a practitioner and manager of flexible packaging product development. While emphasizing materials and applying their features for the benefit of packaged products, he replaced paper and aluminum foil with barrier plastics for modified atmosphere snack food packaging. He managed product development for his long-time employer Printpack Inc. from a narrow \$100 million product line to a broad one of over \$1 billion. He has received lifetime achievement awards from the Food Packaging Division of the Institute of Food Technologists; the Polymers and Laminations Division of the Technical Association of the Pulp and Paper Industry; and the (US) Packaging Hall of Fame. His BA and MS degrees are from Yale University.

Dr. Luyi Sun, President of the Chinese American Society of Plastics Engineers.

Dr. Sun pioneered the injection stretch blow molding (ISBM) of polyolefins. His research led to more than 10 U.S. and international patents and patent applications. Dr. Sun's innovations helped promote the industrial application of polyolefin ISBM. Dr. Sun also conducted leading research in polymer composites and nanocomposites. His patent pending nanocoating technology has led to significant improvement in barrier and flame retardant properties. Dr. Sun is the current President of the Chinese American Society of Plastics Engineers. He has participated in the organization of the International Polyolefins Conference for over 10 years, as well as other SPE sponsored conferences. Dr. Sun is also a dedicated educator. His courses trained many students who have then moved into the polymer industry. He is a member of the SPE Engineering Properties & Structure Division.



Tom Dunn Accepting the SPE Fellow recognition



Dr. Luyi Sun Accepting the SPE Fellow recognition

Message from the D-44 Chair, Barry Morris

I am excited to be the chair of the Flexible Packaging Division for the coming year. I would like to thank our outgoing chair, Paul Zerfas, for keeping us on track during the past year. Our mission is to provide and promote education in the science and technology of flexible packaging. The recently completed ANTEC, highlighted in this newsletter, as well as the upcoming FlexPackCon conference in October are two established examples of this endeavor. These are wonderful networking and educational opportunities and I hope you take full advantage of them. This coming year we also will be organizing a session at the SPE Polyolefins conference in February and working towards establishing a scholarship for packaging students.

I want to welcome our newest board member, Judy Webb. Judy recently joined Sasol North America after being at Nova Chemicals for several years. I also want to thank our outgoing board members, Jim Huang and Carey Yang. Jim is a founding member of the division, a past chair, and most recently the ANTEC technical program chair. Carey has brought his energy to helping organize the upcoming FlexPackCon conference as technical program chair.

FlexPackCon 2016

A blue-themed poster for the SPE FlexPackCon 2016 event. The text is centered and reads: "SPE FlexPackCon 2016", "The Peabody - Memphis, TN", "October 9-12, 2016", and "4spe.org/flexpackcon2016". At the bottom, there is a large "FlexPackCon 2016" logo with the SPE logo to its right. A small note at the bottom states: "* Co-hosted with AIMCAL Web Coating & Handling Conference".

PREDICTING THE IMPACT PUNCTURE RESPONSE OF MULTILAYER FLEXIBLE FOOD PACKAGES USING EXPLICIT FINITE ELEMENT MODELS

Leopoldo A. Carbajal, Rong Jiao, Diane M. Hahm, Barry A. Morris, Randy R. Kendzierski, DuPont
Abstract

In previously presented work (ANTEC 2015), the authors developed a laboratory test method capable of ranking the impact puncture resistance (IPR) of multilayer flexible packages. This paper describes the development of nonlinear finite element models capable of predicting the IPR of the same multilayer structures. Information about the method used to obtain material properties at relevant strain rates, and comparisons between predicted and experimental responses are presented.

Introduction

Impact punctures from falling product during filling operations is a leading cause of package failure, resulting in loss of product freshness. In previous work [1], the authors developed the empirical capabilities to measure and rank the IPR of flexible packages. DuPont's plan is to complement this work with numerical models. Nonlinear finite element models are being developed to help gain a deeper understanding of the relative contribution of individual material properties or geometric choices on the overall IPR of a multilayer structure. It is expected that these models will help identify material arrangements that result in higher IPR, and key material properties that need to be tailored for a particular application and design. In addition to this, the use of numerical models will help to substantially reduce the time and cost it takes to develop an effective package design for a given application.

To evaluate the ability of the models to predict the IPR of multilayer flexible packages, the model results are compared with those presented in reference 1. In that study, the IPR of seven multilayers structures were evaluated using two types of impact tests. The first evaluation was performed using a reverse normal puncture (RNP) test at constant speed (4.235 m/s). The second evaluation consisted of a normal impact drop test conducted at different striking velocities [2.00 m/s to 3.00 m/s] using bullet projectiles (0.223 Remington Full Metal Jacket).

As mentioned in the referenced paper, the structures were made in-house using a 9-layer Macro Engineering blown film line. The structures considered for the study were made using five layers: (HDPE-Tie-Nylon-Tie-Sealant). Details of the compositions of the samples are provided in Tables I, II and III.

Table I: Resins used in study

Resin	Supplier	Grade	Description
HDPE1	Chevron Phillips	9659	0.962 g/cc density, 1 MI
Tie Conc.	DuPont	Bynel® 41E710	Anhydride modified PE
LLDPE1	Dow	Affinity 1880G	mPE, 0.902 g/cc
Nylon1	BASF	Ultramid C	PA 6/6,6
EVA1	DuPont	Elvax® 3174SHB	EVA (18% VA)
Ionomer1	DuPont	Surlyn® 1650B	Zn-ionomer
Ionomer2	DuPont	Surlyn® E185SB	Ionomer
SB1	DuPont	Elvax® CE9619-1	Slip & antiblock concentrate
SB2	DuPont	Conpol™ 5B10S1	Slip & antiblock concentrate

Table II. Flexible Structures compositions

Short Name	Moisture Barrier	Tie Layer	Barrier	Tie Layer	Seal Layer Blend
1	HDPE1	LLDPE1 + 15% Tie Conc	Nylon 1	LLDPE1 + 15% Tie Conc	Typical combination of EVA1, Ionomer1 and SB1 used in commercial films
1A	Same as 1	Same as 1	Same as 1	Same as 1	Same as 1
1B	Same as 1	Same as 1	Same as 1	Same as 1	Same as 1
1C	Same as 1	LLDPE1	Same as 1	Same as 1	Same as 1
2	Same as 1	Same as 1	Same as 1	Same as 1	97% Ionomer2 + 3%SB2
2A	Same as 1	Same as 1	Same as 1	Same as 1	Same as 2
2B	Same as 1	Same as 1	Same as 1	Same as 1	Same as 2

Table III. Layer Thickness (as % of total thickness)

Short Name	Thickness of the Structure (µm)	Moisture Barrier (%)	Tie Layer (%)	Barrier (%)	Tie Layer (%)	Seal Layer Blend (%)
1	55	73.25	2.10	5.65	2.10	16.90
1A	75	67.80	3.79	6.95	4.08	17.38
1B	83	64.02	3.26	18.37	1.89	12.46
1C	72	71.33	2.80	10.28	1.87	13.72
2	65	72.55	1.51	7.51	1.87	16.56
2A	74	70.43	2.83	11.33	1.57	13.84
2B	80	65.54	2.79	17.70	2.17	11.80

Model Introduction

Impact events considered in this study usually have a short dynamic response time, large local deformations and failure of some or all the materials involved. The short duration of the event can be clearly appreciated in Figure 1a. Here a wheat snack cracker is dropped onto a film simulating a vertical-form-fill-seal operation. The image sequence shows that the entire event duration (from impact until the wheat snack cracker is arrested) is less than 10 milliseconds. The nature of the permanent deformation and the failure of the structure can be observed in Figure 1b. The image is a micrograph of the impacted zone for an impact velocity of 6.3 m/s that resulted in penetration. As it can be seen in this figure, the failed zone

is relatively small (the horizontal dimension of the failed zone is less than 0.5mm).

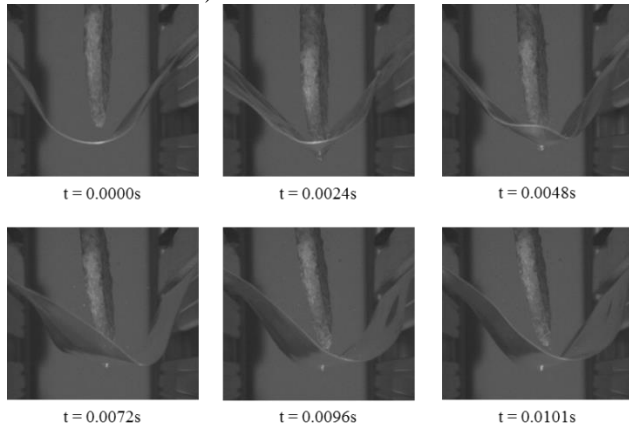


Figure 1a: Cracker drop test deformation sequence captured from high-speed video studies.



Figure 1b: Impact Zone Detail (impact Velocity: 6.3 m/s).

Figure 1: Impact event characteristics.

It is because of these characteristics that the commercial software Abaqus/Explicit is used for the development of the models. An explicit central-difference time integration is utilized. The explicit operator satisfies the dynamic equilibrium equations at the beginning of the increment, t ; the computed accelerations at time t are used to calculate the velocities at time $t + \Delta t/2$ and the displacements at time $t + \Delta t$. The equations of motion are integrated using the explicit central-difference integration rule

$$\dot{u}_{(i+\frac{1}{2})}^N = \dot{u}_{(i-\frac{1}{2})}^N + \frac{\Delta t_{(i+1)} + \Delta t_{(i)}}{2} \ddot{u}_{(i)}^N \quad (1)$$

$$u_{(i+1)}^N = u_{(i)}^N + \Delta t_{(i+1)} \dot{u}_{(i+\frac{1}{2})}^N \quad (2)$$

where u^N is a degree of freedom (displacement or rotational component) and the subscript i refers to the increment number. This integration is explicit in the sense that the kinematic state is advanced using the velocity and the acceleration of the

previous increment. The key to the computational efficiency is the use of diagonal element mass matrices (see Abaqus manuals for more details [2]).

Since the models are expected to provide insight about the contribution of individual material properties and/or geometric selections to the overall IPR of the multilayer structure, it is necessary to consider each material explicitly. Figure 2 shows the level of detail in the thickness direction for the two impact events considered in this paper.

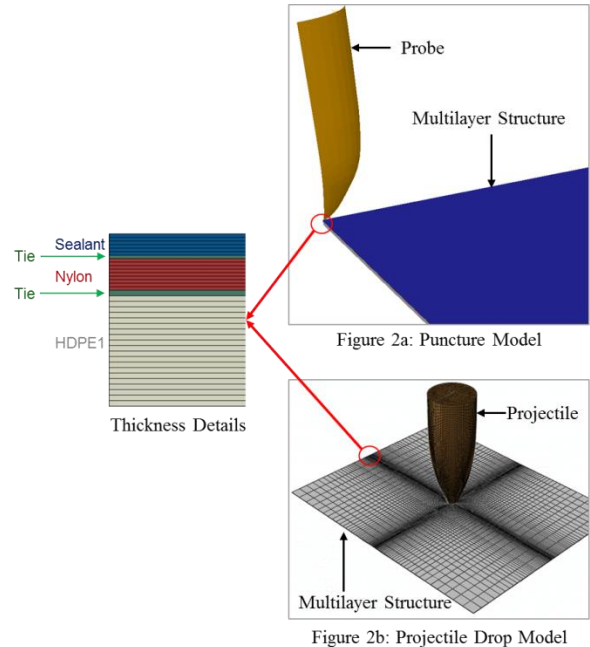


Figure 2: Finite element models details.

As it is shown in Figure 2, three-dimensional finite element models were built using solid elements with reduced integration and hourglass control (C3D8R) for the different layers of the flexible structures. Since the projectile and the stainless steel needle used are much stiffer and stronger than the flexible structures, they are assumed to be perfectly rigid and are idealized using rigid shell elements (all their geometric shapes and dimension are preserved). In both models, the time incrementation scheme used was “Element by Element”. This conservative scheme uses a stability limit based on the highest element frequency in the entire model, and the element-by-element estimate is determined using the current dilatational wave speed in each element.

To reduce computational effort, all models take advantage of the symmetry of the impact tests and only one quarter of the problem is considered. In all calculations, the total “artificial” strain energy was less than 10% of the total elastic and plastic energy (large values of artificial strain energy indicate that mesh

refinement or other changes to the mesh are necessary to improve model accuracy).

Obtaining Material Properties

The procedure used to obtain material properties for each of the layers of interest consisted of a two-step process. The first part of the process entailed conducting tensile tests of each individual layer at two different strain rates: $0.001s^{-1}$ and $1.00s^{-1}$. Mathcad with the Kornucopia® toolbox was used to process and convert all the raw force-displacement data into true stress and strain. Figure 3 shows the basic test setup used for this part of the procedure.

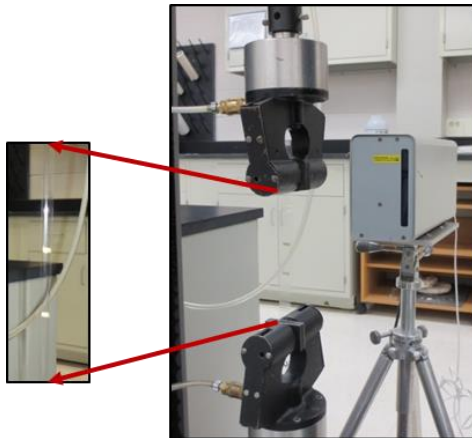


Figure 3: Tensile test basic setup.

The second part of the procedure consisted of performing a reverse impact test for the individual material layers which is similar to the puncture test for multiple layer films described in a previous paper [1]. Based on the experience gained by the authors while developing the referred test method [1], the same needle profile and impact speeds (4.235 m/s) were used for this test. Figure 4 shows the profile of needle used.

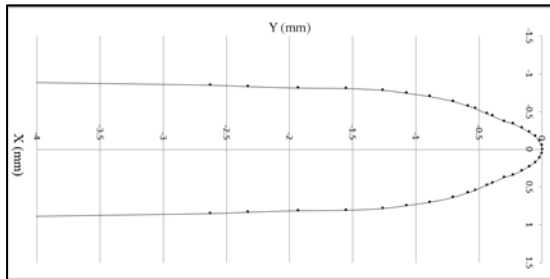


Figure 4: Puncture needle profile.

Figure 5 shows the reverse puncture test setup. As it was the case of reference 1, the signals collected consisted of displacement (LVDT), load, trigger signal generated by the data acquisition system (used to activate two high speed cameras), and one exposure strobe signal output for each camera. Both cameras acquire images at a rate of 50,000

frames/s and were set to operate in a master-slave mode. The DAQ system has an effective sampling rate (sampling rate after the application of AA filters) of 500,000 samples/s for each of the 5 data channels used

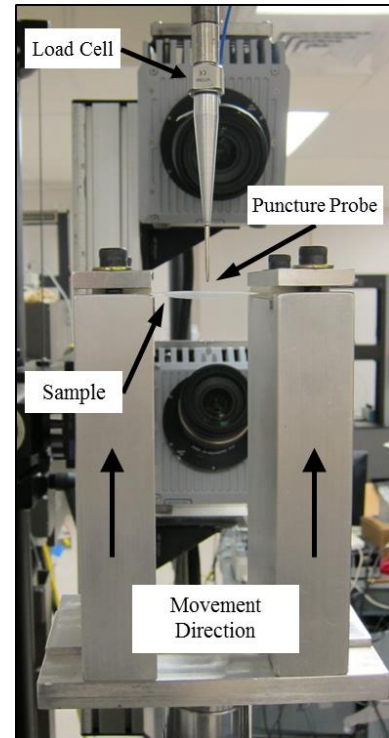


Figure 5: Reverse impact puncture test assembly.

Mathcad with the Kornucopia® tool box was used to post process the force-displacement data. Numerical integration of the experimental data was performed to obtain work-displacement curves.

The final step to obtain the material properties consisted of creating a numerical model of the puncture test for individual layers. Using the material properties obtained in the tensile tests, an initial force-displacement response is predicted and compared with the experimental responses. Following an iterative process, small modifications are made to the damage initiation criteria and the material properties until the predicted response matches the average experimental response. The refined properties are those corresponding to the best prediction.

This procedure was used to obtain all materials properties needed to predict the IPR of the multilayer flexible packages shown in the previous paper [1]. As an example, Figure 6 compares the experimental and predicted work-displacement responses for Nylon1. Work is used because the act of integrating the experimental (and numerical) force signal over the displacement signal reduces the noise.

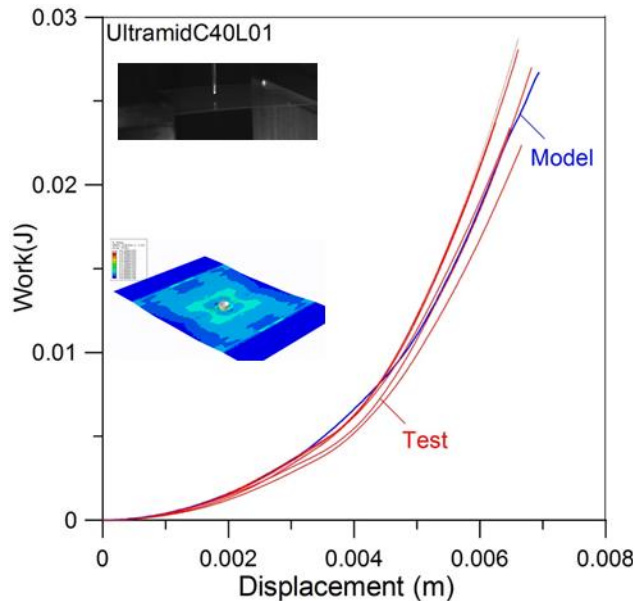


Figure 6: Experimental and predicted work-displacement responses for nylon1.

Multilayer Level Predictions

Two impact events are considered to assess the ability of the models to predict the IPR of the multilayer structures. The first set of predictions corresponds to the RNP impact event. Figure 7 shows a sequence of images depicting typical deformed shapes observed during the simulation of the RNP event. These agree qualitatively with high speed video images from the actual experiment.

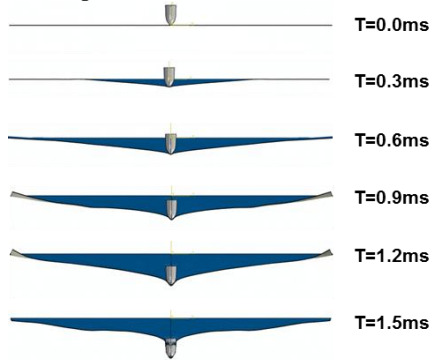


Figure 7: Typical predicted deformed shapes.

Figure 8 compares the predicted and experimental ultimate work for all seven structures characterized in reference 1. Average material properties were used to predict the response of all structures.

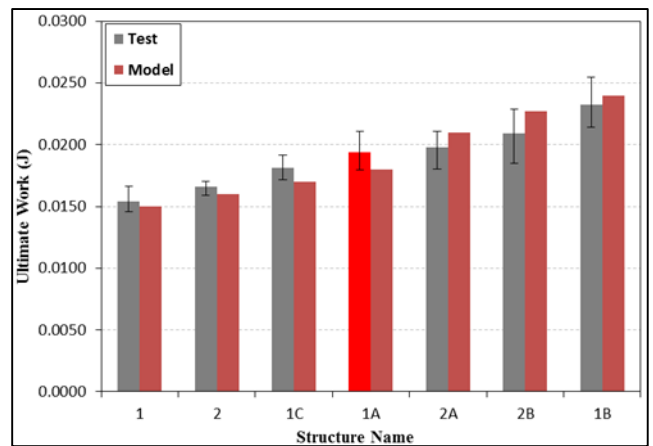


Figure 8: Experimental and predicted ultimate work

As it can be observed in Figure 8, the model and the test method rank the structures in exactly the same order. When judging the accuracy of the prediction, the largest registered error between predicted and the average experimental results is 8.5% (structure 2B), and the average error for all structures is 5.4%. These values are considered acceptable for this type of simulation. As stated in reference 1, the ranking in Figure 8 could be explained largely by the amount of nylon present in the structures. Figure 9 shows the explicit relationship between the nylon thickness and the ultimate work of the structure.

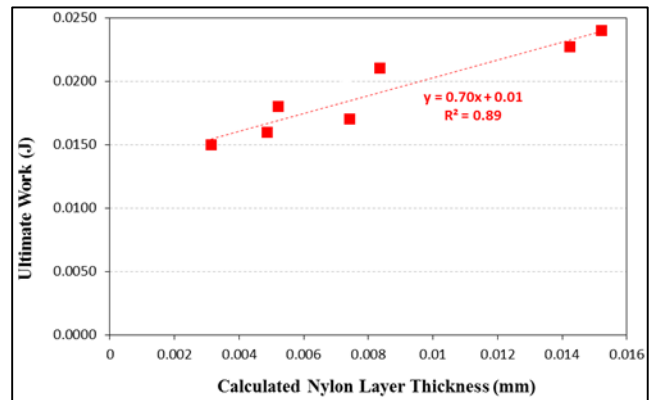


Figure 9: Predicted ultimate work and nylon thickness

In reference 1, the point corresponding to structure 1A was excluded from the linear regression. This was done because its ranking did not correspond with the intended (design) nylon thickness. During this publication, it was found that the actual thickness was higher than the intended value. Using this value, the model was able to rank the structure in the same place as the experiment.

The second set of predictions corresponds to the bullet drop impact event. Figure 10 shows the deformed predicted shapes as seen from the back face of structure 1B for a velocity that ultimately resulted in puncture. Figure 10a corresponds to an instant just before the puncture, and Figure 10b corresponds to the instant when the projectile has penetrated the structure.

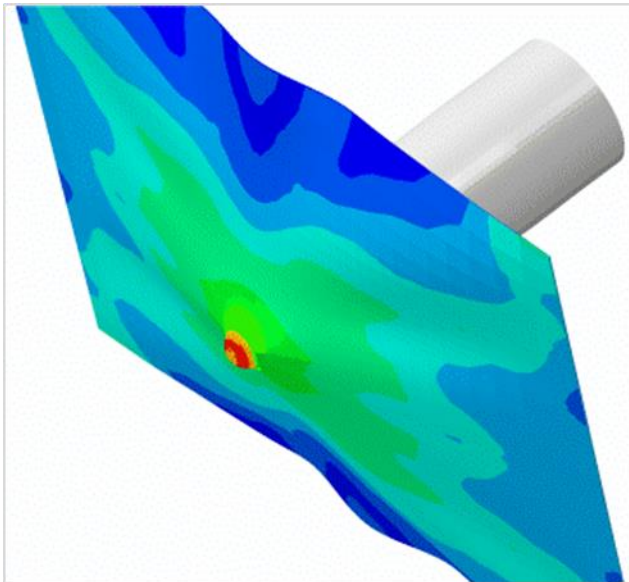


Figure 10a: Instant before penetration

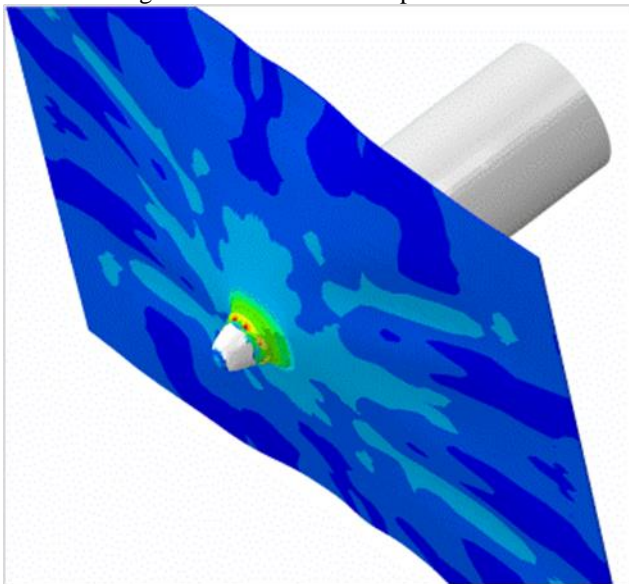


Figure 10b: Instant after penetration

Similar to the corresponding test, in this simulation the bullet is assigned an initial velocity and then the model predicts if the structure can arrest the projectile. All predictions were performed using average material properties. Figure 11 compares the experimental and predicted V50s (the velocity at which 50% of the projectiles would puncture the structure) for six of the seven structures. All predictions needed to calculate

the puncture velocity of structure 1 were not finished at the time of writing this paper.

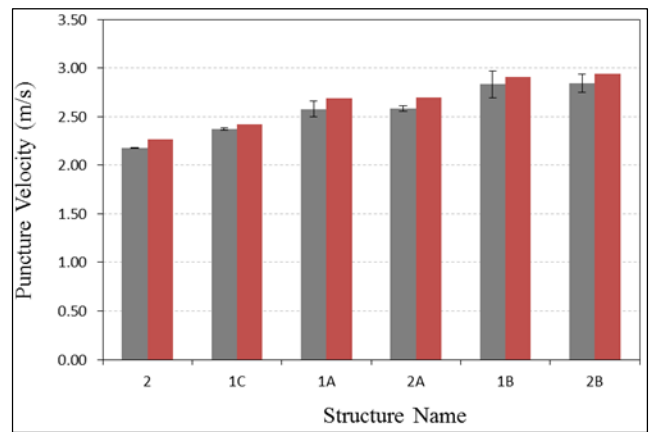


Figure 11: Experimental and predicted puncture velocities

The model and the test rank the structures in exactly the same order. When assessing the accuracy of these predictions, the largest registered error between predicted and the average experimental results is 4.5% (structure 2A), and the average error for all structures is 3.6%. These values are considered acceptable for this type of simulation.

Conclusions

A practical procedure has been developed for predicting the IPR of multilayer flexible packages using numerical models and the mechanical properties of the materials involved. Model predictions for seven multilayer flexible packages and two types of events were conducted. As it can be observed in Figures 8 and 11, all predictions are in close agreement with the experimental data. Future publications will cover further validation of this capability, and its use to design higher impact resistance flexible packages.

References

1. Leopoldo A. Carbajal, Rong Jiao, Diane M. Hahm, Barry A. Morris, Randy R. Kendzinski, "Impact Puncture Resistance of Multilayer Flexible Food Packages," ANTEC®, Orlando, FL, March 2015.
2. Abaqus 6.13 Documentation, Dassault Systemes, Providence, RI, USA.